Growth and characterization of small band gap (~0.6 eV) InGaAsN layers on InP

Milind R. Gokhale, Jian Wei, Hongsheng Wang, and Stephen R. Forrest
Department of Electrical Engineering, Center for Photonics and Optoelectronic Materials (POEM), Princeton University, Princeton, New Jersey 08544

(Received 21 October 1998; accepted for publication 4 January 1999)

We demonstrate the growth of small band gap ($E_g \sim 0.6$ eV) strained and lattice matched single crystal InGaAsN alloys on InP substrates. InGaAsN layers with N concentrations varying from 0.6% to 3.25% were grown by gas source molecular beam epitaxy using a radio frequency plasma nitrogen source. Lattice-matched, 0.5-μm-thick InGaAsN layers with smooth surface morphologies and abrupt interfaces were achieved. Low temperature photoluminescence measurements reveal a band gap emission wavelength of 1.9 μm (at 20 K) for lattice matched InGaAsN (N~2%). Tensile strained $In_{0.53}Ga_{0.47}As/In_{0.53}Ga_{0.47}As_{0.994}N_{0.006}$ multiple quantum wells emitting at 1.75 μm at 20 K are also reported. © *1999 American Institute of Physics.* [S0003-6951(99)04109-1]

InGaAsP alloys grown lattice matched to InP substrates are widely used as materials for lasers and detectors at optical fiber communication wavelengths.[1,2] For detectors, the long wavelength cutoff is $\lambda_{CO}=1.7$ μm, determined by the band gap of the lattice-matched $In_{0.53}Ga_{0.47}As$ absorption layer.[3] The cutoff wavelength for InGaAsP-based lasers is 2 μm, limited by the maximum compressive strain that can be accommodated in InGaAs quantum wells forming the active region.[4] Detectors with response extending beyond 1.7 μm have been fabricated using In-rich lattice-mismatched InGaAs layers.[5] However, higher dark currents due to defects in the relaxed, lattice-mismatched InGaAs layer and the need to have compositionally graded buffer layers to reduce dislocations make detectors with lattice matched absorbing layers a potentially superior approach.[6] In this work, we demonstrate that strained and lattice-matched InGaAsN alloys on InP can extend the wavelength of photonic device operation beyond that accessible to the InGaAsP/InP system.

Recently, it was proposed that the addition of a small fraction of nitrogen into group III arsenides and phosphides results in a material (called a mixed nitride) with a smaller band gap than the corresponding binary compound.[7] A large band gap bowing parameter due to the high electronegativity of nitrogen is believed to be responsible for this unusual property of mixed nitrides.[7] Subsequently, numerous experimental reports of a reduction in band gap for various nitrogen containing ternary alloys have been published.[8–12] Recently, InGaAsN based light sources such as 1.3 μm wavelength lasers[13,14] and 1.45 μm wavelength light emitting diodes[14] were demonstrated on GaAs substrates. Compared to growth on GaAs, reports of mixed nitride growth on InP substrates are limited. Nitrogen fractions up to 1% were reported in $InN_{1-x}P_x$/InP layers grown by gas source molecular beam epitaxy (GSMBE).[15] Also, quantum wells employing InNAsP with emission in the 1.1–1.5 μm wavelength range have been reported.[16]

Based on the bowing parameter for GaN_xAs_{1-x}[7] and InN_xAs_{1-x},[17] we have calculated the band gap of InGaAsN alloys on InP. The band gap data were extrapolated using Vegard's law from experimental and calculated data for the four ternary compounds, namely InGaAs,[18] GaInN,[7] GaNAs,[7] and InNAs.[17] The band gap cutoff wavelengths of $In_xGa_{1-x}As_{1-y}N_y$ alloys shown in Fig. 1 are plotted along contours corresponding to compositions required to achieve either lattice matched or strained layers on InP.[18] From the plot, we find that for N concentrations as low as 4%, we anticipate wavelength cutoffs of 2.0 μm, extending to 2–5 μm for higher nitrogen concentrations. Compressively strained layers employed in quantum wells may extend the wavelength of InP-based lasers into the 2–3 μm range. At N>12% the band gap drops rapidly to zero as InGaAsN becomes semimetallic.

To test the predictions of Fig. 1, InGaAsN alloys with varying N concentrations were grown by GSMBE on semi-insulating (100) InP substrates.[19] Group V elements were obtained by thermally cracking PH_3 and AsH_3 at 900 °C. To generate the active N species, ultrahigh purity nitrogen gas was introduced via a mass flow controller into a radio frequency (rf) plasma source.[20] After oxide desorption from the substrate at 500 °C, a 0.2-μm-thick InP buffer layer was grown at 480 °C. The growth was interrupted and the sample

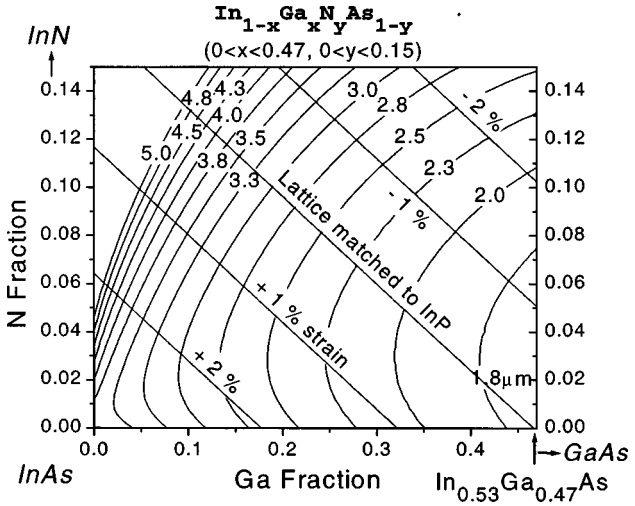

FIG. 1. Band gap cutoff wavelength ($\lambda>1.7$ μm) and lattice constant for InGaAsN alloys mixed as a function of N and Ga atomic fraction.

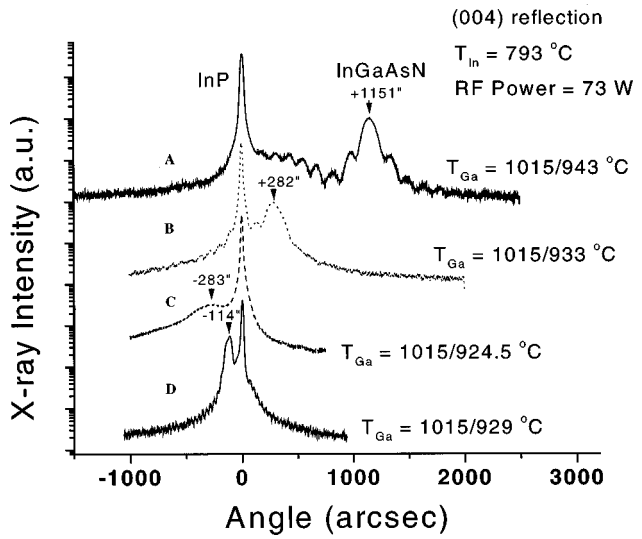

FIG. 2. Double crystal x-ray rocking curves (004 reflection) of a series of InGaAsN samples grown at fixed In and N fluxes, but a varying Ga flux obtained by changing base temperature on the Ga Knudsen cell while maintaining tip temperature at 1015 °C.

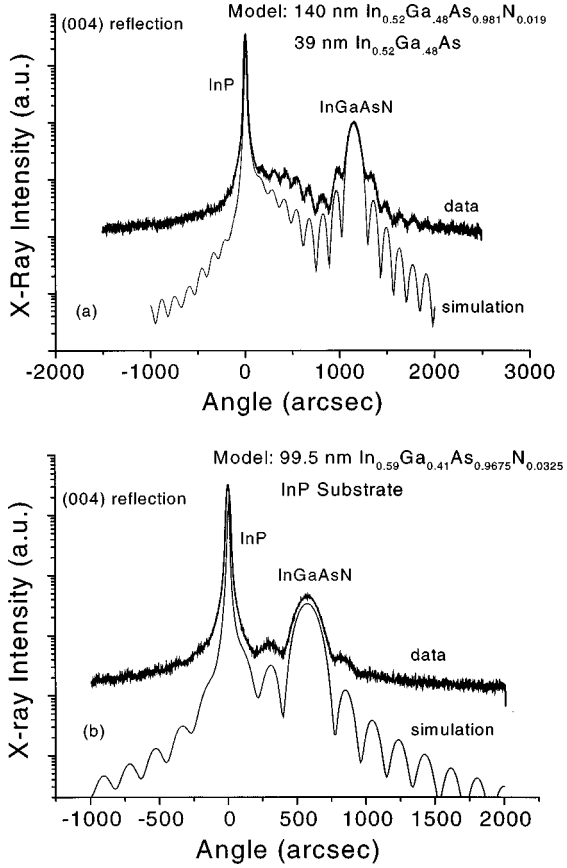

FIG. 3. Use of dynamical x-ray simulation analysis to estimate the nitrogen fraction in InGaAsN. The simulation (thin lines) was fit to the data (bold lines) using known In/Ga fraction and growth rates.

temperature reduced to 320–370 °C under an AsH_3 over pressure. Then a high-brightness nitrogen plasma was initiated, and the N_2 flow and rf power (65–125 W) were adjusted to achieve the desired N/As ratio, at a constant AsH_3 flow of 1.5 sccm. A 514 nm wavelength, Ar-ion laser and a closed cycle helium cooling system were used for low temperature photoluminescence (PL) measurements of the epitaxial layers. Transmission measurements were performed using a tungsten-halogen source used in combination with a Fourier transform infrared (FTIR) spectrometer.

A series of InGaAsN samples were grown with a range of In/Ga ratios adjusted by keeping the In Knudsen cell temperature and N flux (0.06 sccm at 73W rf power) constant, while varying the Ga fraction by changing the base temperature of a dual-filament Ga Knudsen cell. For sample A (see Fig. 2), the In/Ga ratio was 0.52:0.48 determined from x-ray analysis of an InGaAs (no N) sample. The well-defined peak at 1151″ on the tensile side (−0.9% strain) of the InP substrate peak indicates growth of a single crystal InGaAsN film. Upon reducing the Ga cell temperature by ~10 °C (thereby increasing the In/Ga ratio) the strain was reduced to −0.3% as indicated by a shift in the InGaAsN peak towards that of InP. Reducing the Ga fraction further, the peak corresponding to InGaAsN shifts from tensile to compressive (−283″). A final adjustment in Ga-cell temperature allowed us to grow a 0.5-μm-thick $In_{0.59}Ga_{0.41}As_{0.981}N_{0.019}$ lattice matched layer with a mismatch $\Delta a/a < 9\times10^{-4}$, where a is the InP lattice constant. In a similar manner, a lattice-matched sample with ~1% N was also grown with $\Delta a/a < 4\times10^{-4}$. The lattice-matched samples exhibited a smooth surface morphology similar to InP layers, with no surface roughening visible using a Nomarski microscope. X-ray rocking curves of the lattice matched samples showed Pendellosüng fringes in InGaAsN layers >0.5 μm thick (sample D, Fig. 2), indicating an atomically flat InGaAsN/InP interface and top surface. A streaky reflection high energy electron diffraction (RHEED) pattern observed during growth also suggests a two-dimensional layer-by-layer growth mode.

The nitrogen fraction was determined by dynamical x-ray analysis of the rocking curves assuming Vegard's law and lattice constants corresponding to zinc blende InN and GaN. For sample A [Fig. 3(a)], the full-width at half-maximum (FWHM) of the InGaAsN peak and location of each Pendellosüng fringe match well with the model derived from the known growth conditions. Also shown in Fig. 3(b) is a strained InGaAsN layer grown with higher rf power (~95 W) but the same N flow and In/Ga ratio as sample D. This results in a nitrogen concentration of 3.25%, which was the maximum value achieved. To confirm N incorporation, InGaAs/InGaAsN multiple quantum wells (MQW) were grown with the same In/Ga ratio in the wells and barriers, the only difference being that during the growth of the InGaAsN well layers, the shutter of the nitrogen cell was opened. A 10 period $In_{0.535}Ga_{0.465}As_{0.994}N_{0.006}/In_{0.535}Ga_{0.465}As$ MQW sample with 200-Å-thick wells and 300-Å-thick barriers was grown at a substrate temperature of 350 °C. Since the barrier and well had the same In/Ga ratio, the clear satellite peaks seen in the x-ray data confirmed the periodic incorporation of N.

Figure 4 shows low temperature (T=20 K) photoluminescence measurements for the MQW and two lattice matched InGaAsN samples. The peak wavelength for the lattice-matched samples shifted from 1.78 to 1.91 μm, and the intensity decreased with increasing N concentration. The

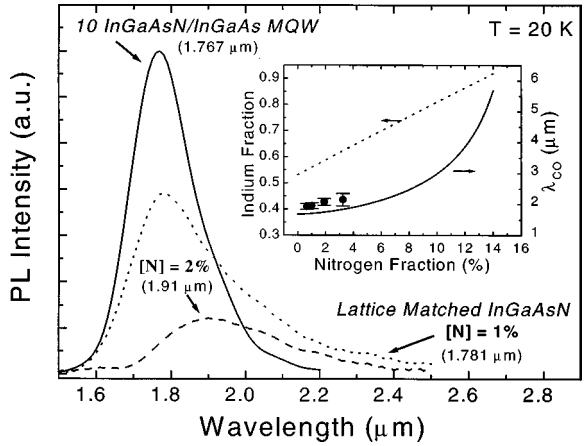

FIG. 4. Low temperature photoluminescence spectra of MQW and lattice matched InGaAsN samples. Inset: band gap cutoff wavelength extrapolated to room temperature taken from PL data (points) as a function of nitrogen concentration. Also shown is our calculated estimate of the cutoff wavelength taken from Fig. 1.

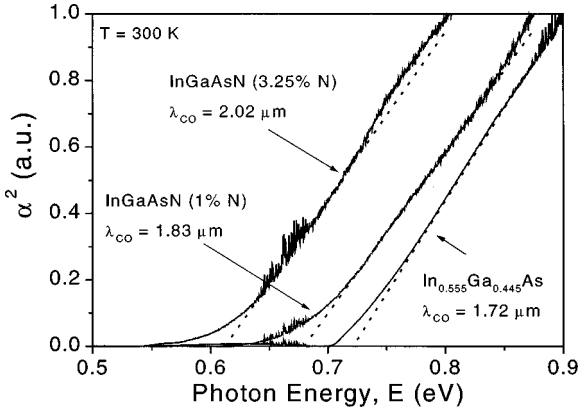

FIG. 5. Room temperature transmission spectra for InGaAsN layers with ~1% and 3% N concentration, showing a red shift in transmission edge relative to a strained $In_{0.555}Ga_{0.445}As$ sample. Maximum band gap cutoff wavelength extrapolated from data is $\lambda_{CO}=2.02$ μm.

tensile strained MQW sample showed the strongest PL peaked at 1.75 μm. For these samples, no detectable room temperature photoluminescence was obtained, indicating the presence of a high concentration of nonradiative centers. Low temperature PL for the lattice matched samples also showed a long emission tail below the band gap. A similar feature has previously been observed in InGaAsN/GaAs QWs with 1% to 3% N concentration.[21] The low luminescence efficiency of these samples is in contradiction to the excellent structural quality indicated by an atomically smooth surface and narrow x-ray peaks (FWHM $<60''$). These defects may be due to vacancies induced by the low growth temperature, or may be due to residual strain introduced by the small diameter N atom in a group V site. The inset in Fig. 4 shows the band gap cutoff wavelength at room temperature as a function of nitrogen concentration. The data points were extrapolated from the low temperature PL measurements by including a 60 meV reduction in band gap, assuming a temperature dependence similar to $In_{0.53}Ga_{0.47}As$.[22] The solid line is taken from the calculations in Fig. 1. We attribute the large red shift in the data as compared to predictions to inaccuracies in our linear interpolation method, or to residual lattice strain. Optical transmission spectra confirm the red shift in the band edge of InGaAsN alloys relative to $In_{0.555}Ga_{0.445}As$. Figure 5 shows the square of the absorption coefficient (α^2) as a function of the incident photon energy (E), for $In_{0.555}Ga_{0.445}As$ and InGaAsN samples with 1% and 3% nitrogen. The band gap given by the intercept with the abscissa increases monotonically with N content.

In summary, we have grown InGaAsN alloys by GSMBE with high structural quality on InP substrates. For a constant nitrogen flow, the N concentration in the films was found to be proportional to the rf power. Lattice matched and strained samples with In/Ga ratios greater than 0.53:0.47 and a nitrogen concentration as high as 3.25% were demonstrated with a band gap cutoff wavelength of 2.02 μm (~0.6 eV). Low temperature PL measurements indicate that the emission intensity is reduced and the FWHM is increased with N concentration. These results demonstrate the potential of strained and lattice matched InGaAsN layers grown on InP for significantly extending the wavelength range of the InGaAsP/InP material system.

The authors gratefully acknowledge DARPA (Ray Balcerak) for support of this work. They also thank Greg Olsen and Marshall Cohen of Sensors Unlimited for helpful discussions.

[1] Y. Suematsu, Proc. IEEE **71**, 692 (1983).
[2] W. T. Tsang, M. C. Wu, T. Tanbun-Ek, R. A. Logan, S. N. G. Chu, and A. M. Sargent, Appl. Phys. Lett. **57**, 2065 (1990).
[3] *Semiconductor and Semimetals*, edited by W. T. Tsang (Academic, New York, 1985), Vol. 22.
[4] S. Forouhar, S. Keo, A. Larsson, A. Ksendzov, and H. Temkin, Electron. Lett. **29**, 574 (1993).
[5] G. H. Olsen, A. M. Joshi, S. M. Mason, K. M. Woodruff, E. Mykietyn, V. S. Ban, M. J. Lange, J. Hladky, G. C. Erickson, and G. A. Gasparian, Proc. SPIE **1157**, 2263 (1989).
[6] J. C. Dries, M. R. Gokhale, K. J. Thomson, and S. R. Forrest, Appl. Phys. Lett. **73**, 2263 (1998).
[7] S. Sakai, Y. Ueta, and Y. Terauchi, Jpn. J. Appl. Phys., Part 1 **32**, 4413 (1993).
[8] M. Weyers and M. Sato, Appl. Phys. Lett. **62**, 1396 (1993).
[9] M. Kondow, K. Uomi, K. Hosomi, and T. Mozume, Jpn. J. Appl. Phys., Part 2 **33**, L1056 (1994).
[10] Y. Qiu, A. Nikishin, H. Temkin, N. N. Faleev, Yu. A. Kudriavtsev, Appl. Phys. Lett. **70**, 3242 (1997).
[11] W. G. Bi and C. W. Tu, Appl. Phys. Lett. **70**, 1608 (1997).
[12] H. Naoi, Y. Naoi, and S. Sakai, Solid-State Electron. **41**, 319 (1997).
[13] M. Kondow, T. Kitatani, S. Nakatsuka, M. Larson, K. Nakahara, Y. Yazawa, M. Okai, and K. Uomi, IEEE J. Sel. Top. Quantum Electron. **3**, 719 (1997).
[14] S. Sato, Y. Osawa, and T. Saitoh, Jpn. J. Appl. Phys., Part 1 **36**, 2671 (1997).
[15] W. G. Bi and C. W. Tu, J. Electron. Mater. **26**, 252 (1997).
[16] W. G. Bi and C. W. Tu, Appl. Phys. Lett. **72**, 1161 (1998).
[17] T. Yang, S. Nakajima, and S. Sakai, Jpn. J. Appl. Phys., Part 2 **36**, L320 (1993).
[18] R. L. Moon, G. A. Antypas, and L. W. James, J. Electron. Mater. **3**, 635 (1974).
[19] RIBER 32 MBE, RIBER 92503 Rueil Malmaison Cedex, France.
[20] UNI-BULB RF source, EPI MBE Products Group, St. Paul, MN.
[21] H. P. Xin and C. W. Tu, Appl. Phys. Lett. **72**, 2442 (1998).
[22] S. Adachi, *Physical Properties of III-V Semiconductor Compounds* (Wiley, New York, 1992).